Electronic Supplementary Information (ESI)

Single-Molecule, Single-Particle Observation of Size-Dependent Photocatalytic Activity in Au/TiO_2 Nanocomposites

Nan Wang,[†,‡] Takashi Tachikawa,[†] and Tetsuro Majima[*†]*

[†] The Institute of Scientific and Industrial Research (SANKEN), Osaka University, Mihogaoka 8-1, Ibaraki, Osaka 567-0047, Japan and [‡] College of Chemistry and Chemical Engineering, Huazhong University of Science and Technology, Wuhan, 430074, P.R. China

*e-mail: tachi45@sanken.osaka-u.ac.jp (T.T.); majima@sanken.osaka-u.ac.jp (T.M.)

Contents

S1. Experimental methods

Materials. 8-(3,4-Dinitrophenyl)-1,3,5,7-tetramethyl-4,4-difluoro-4-bora-3a,4a-diaza-s-indacene (DN-BODIPY) was synthesized according to the procedures reported in the literature.[1] Au/TiO_2 particles were prepared by the deposition-precipitation method under various heating temperatures and times as described elsewhere.[2] The details of the procedures and characterizations are given in the following sections.

Instruments. Transmission electron microscopy (TEM) measurements were performed using a Hitachi H-9000 instrument equipped with a tilting device operating at 300 kV. Steady-state UV–visible absorption and diffuse reflectance spectra were measured with UV–visible–NIR spectrophotometers (Shimadzu UV-3100 and Jasco V-570, respectively). Steady-state fluorescence spectra were measured by a Hitachi 850 fluorescence spectrophotometer. All of the experimental data were obtained at room temperature.

Bulk photocatalytic experiments. For typical photocatalytic runs, 1.0 mL of a Au/TiO_2 dispersion (1.0 g L^{-1}) containing DN-BODIPY (50 μM in MeOH) was first sonicated for 2 min, and then transferred into a quartz cuvette sealed with a cap. Prior to UV illumination, the suspension was purged with Ar gas for 10 min to completely remove the dissolved oxygen. The reaction mixture was maintained in suspension using a magnetic stirrer and, simultaneously, Ar gas was purged during the entire UV illumination period. The intensity of the UV light in the photoreactor was measured to be ca. 35 mW cm^{-1}. After stopping the UV illumination, the sample was kept in an Ar atmosphere for 5 min, centrifuged at 6200 rpm (Hitachi, himac CF16RX), and then filtered through a 0.1-μm pore size PTFE filter (Whatman) to remove the particles. The filtrates were collected, diluted to 10% with methanol, and then analyzed using the UV–visible absorption and fluorescence spectrometers.

Sample preparation for single-molecule fluorescence experiments. The cover glasses and slide glasses were purchased from Matsunami Glass and cleaned by sonication in a 20% detergent solution (As One, Cleanace) for 6 h, followed by repeated washings with warm running water for 30 min. Finally, the cover glasses were washed again with Milli-Q ultrapure water (Millipore). Well-dispersed

methanol suspensions of TiO_2 or Au/TiO_2 particles were spin-coated on the cleaned cover glasses. The cover glasses were annealed at 363 K for 30 min to immobilize the particles on the glass surface, and then mounted on the bottom of a stainless steel holder designed for viewing specimens on the microscope. A cleaned cover glass was placed on the particle-coated glass using a 0.5-mm thickness Teflon spacer to form a chamber with an internal volume of about 150 μL. An Ar-saturated sample solution was then introduced into this chamber in an Ar-purged glove box ($[O_2] < 0.5$ vol%) and a cap with an O-ring seal was tightly screwed to prevent the solution from escaping. The oxygen concentration was measured by an oxygen analyzer, maxO_2+ (Maxtec, Inc.).

Single-molecule fluorescence measurements by TIRFM. The experimental setup was based on an Olympus IX71 inverted fluorescence microscope. The details of this experimental setup are described elsewhere.[3, 4] The position and size of the isolated Au/TiO_2 particles immobilized on the cover glass were determined by a transmission image obtained by illuminating the sample from above using a halogen lamp (Olympus, U-LH100L-3) and an atomic force microscope (AFM) image (Asylum Research, MFP-3DBIO). The light emitted from a CW Ar ion laser (Melles Griot, IMA101010BOS; 488 nm, 50 mW) was reflected by a first dichroic mirror (Olympus, RDM450), which reflected wavelengths longer than 450 nm and was transparent to light shorter than 450 nm, toward a second dichroic mirror (Olympus, DM505). The CW laser light passing through an oil objective (Olympus, UPLSAPO 100XO; 1.40 NA, 100×) after reflection at the second dichroic mirror was totally reflected at the cover glass-methanol interface, which generated an evanescent field (the penetration depth from the interface was ca. 200 nm), making it possible to detect a single fluorescent probe on a single Au/TiO_2 particle. The 365-nm light emitted from an LED (OPTO-LINE, MS-LED-365) and passing through an ND filter and the objective was used for the excitation of the TiO_2 or Au/TiO_2 particles. The intensity of light passing through the objective, immersion oil, and cover glass was measured with a power meter (Ophir, Nova II) equipped with a PD300-UV head.

The fluorescence emission from the fluorescent products generated over a single TiO_2 or Au/TiO_2 particle on the cover glass was collected using the same objective, magnified by a 1.6× built-in

magnification changer (thus, net magnification is 160×), and passed through a bandpass filter (Semrock, FF01-531/40-25) to remove the undesired scattered light, and then imaged by an electron-multiplying charge-coupled device (EM-CCD) camera (Roper Scientific, Cascade II:512). The images were recorded at a frame rate of 20 frames s^{-1} and processed using ImageJ (http://rsb.info.nih.gov/ij/) or OriginPro 8.1 (OriginLab). All experimental data were obtained at room temperature.

Single-molecule fluorescence measurements by confocal microscopy. Confocal fluorescence images were taken on an objective-scanning confocal microscope system (PicoQuant, MicroTime 200) coupled to an Olympus IX71 inverted fluorescence microscope. The samples were excited through an oil objective (Olympus, UAPON 150XOTIRF; 1.45 NA, 150×) with a 485-nm pulsed laser (PicoQuant, LDH-D-C-485) controlled by a PDL-800B driver (PicoQuant). The emission was collected with the same objective and detected by a single photon avalanche photodiode (Micro Photon Devices, PDM 50CT) through a dichroic beam splitter, bandpass filter (Semrock, FF01-531/40-25), and 100-μm pinhole for spatial filtering to reject out-of-focus signals. The data collected using the PicoHarp 300 TCSPC module (PicoQuant) were stored in the time-tagged time-resolved mode (TTTR), recording every detected photon with its individual timing, which were used for the single-molecule analysis. All of the experimental data were obtained at room temperature.

Atomic force microscope (AFM) measurements. AFM images were obtained using an MFP-3D-BIO (Asylum Research) mounted on the Olympus IX71 inverted fluorescence microscope. All of the images were obtained using a tapping mode with a silicon cantilever (Olympus, OMCL-AC200TS) at room temperature.

S2. Preparation and characterization of Au/TiO_2

A series of Au nanoparticle-loaded TiO_2 (Au/TiO_2) photocatalysts were prepared by the deposition-precipitation method using $HAuCl_4$ and TiO_2 particles (A-100, Ishihara Sangyo, 100–200-nm particles) as the raw materials.[2] In a typical procedure, the pH of a 4.86-mM aqueous solution of $HAuCl_4•4H_2O$ (20 mL) was adjusted to 6.0 with 1.0 M NaOH, and then the solution was heated to 70 °C. After 2.0 g of

the TiO_2 particles were preheated at 650 °C for 4 h, they were added to this solution and the mixture was magnetically stirred at 70 °C for 1 h. The particles were washed with Milli-Q water three times and then heated in air. Adjusting the heating temperatures (T) and times (t) made it possible to tailor the average diameter of the Au nanoparticles (d_{Au}). All of the different Au/TiO_2 powders had a pink or purple color due to the surface plasmon resonance bands of the Au nanoparticles, which had d_{Au} values ranging from 5.5 to 14.1 nm (Fig. S1A). Fig. S1C shows the Au particle size distributions obtained for the synthesized Au/TiO_2 particles, being similar to Tada's result.[2] The inset shows a typical TEM image. It can be seen that the diameters and shapes of the Au nanoparticles are fairly uniform. According to the literature, the Au nanoparticles are supported on the {101} surface of TiO_2 with an orientation relationship of $Au\{111\}//TiO_2\{101\}$.[5] The XRD patterns of all the Au/TiO_2 samples showed the same diffraction peaks as naked TiO_2 having a highly crystalline anatase phase. No characteristic diffraction peaks assigned to Au were observed, possibly due to the small amount of loaded Au nanoparticles (Fig. S1B). We selected three different sizes for the Au/TiO_2 particles to be used as test samples and denoted these as 5 nm, 8 nm, and 14 nm Au/TiO_2. As the Au particle size increased, the mean number of Au nanoparticles loaded per TiO_2 particle (N_{Au}) significantly decreased.

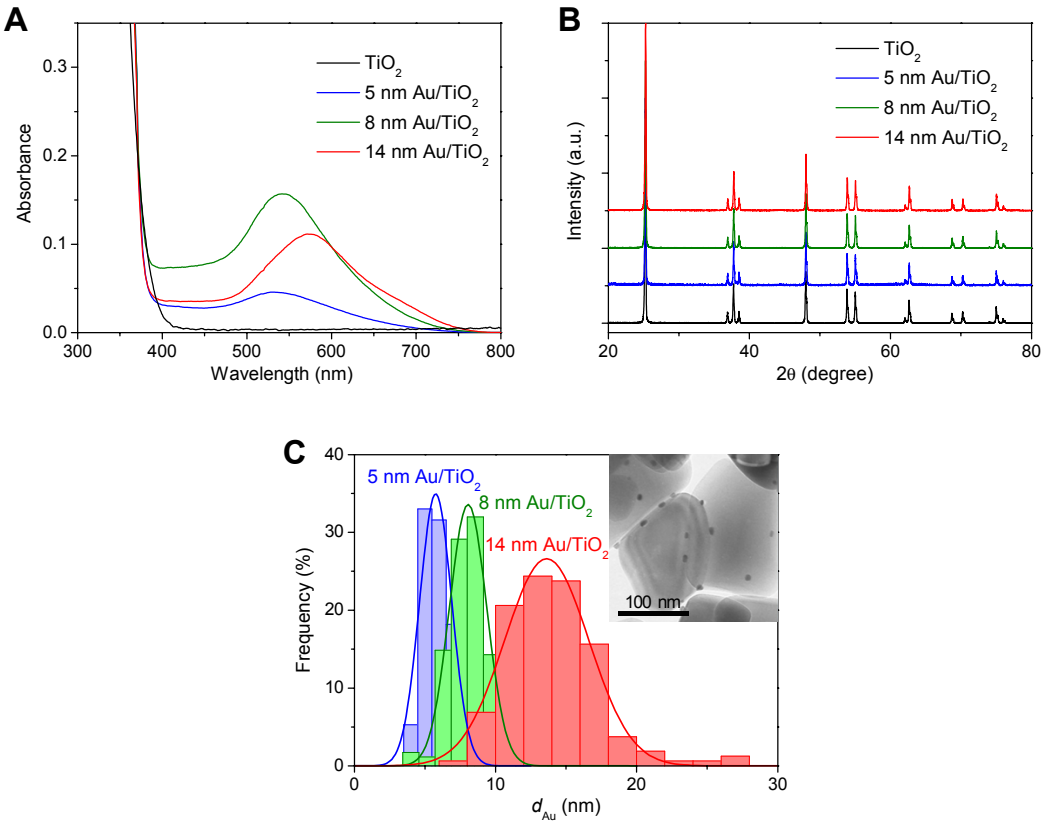

Fig. S1. (A) Diffuse reflectance spectra and (B) XRD patterns of Au/TiO_2. (C) Diameter distributions of Au nanoparticles loaded onto the TiO_2 surface. The inset shows a typical TEM image of 8 nm Au/TiO_2 particles. The size of the TiO_2 particles was ca. 100–200 nm.

S3. Ensemble-averaged photocatalytic activity

The performance and applicability of our probe for the in-situ evaluation of the photocatalytic activity were studied at the ensemble-averaged level. Fig. S2A illustrates the spectral changes during the photocatalytic reduction of DN-BODIPY (50 μM) over 8 nm Au/TiO_2 (1.0 g L^{-1}) in Ar-saturated methanol. It is easily seen that after UV illumination for 10 min, the peak in the absorption spectra was blue shifted. In addition, a new fluorescence peak appeared at ca. 510 nm and its intensity dramatically increased by over several hundred times at 30 min of UV irradiation.

Fig. S2B illustrates the effect of the Au particle size on the photocatalytic activity of the Au/TiO_2 at the given UV illumination time of 30 min. It was found that the photocatalytic activity of the Au/TiO_2 increased as the Au nanoparticle size was increased from 5.5 to 8.1 nm, and then slightly decreased when the Au nanoparticle size continued to increase. This is consistent with the tendency reported in the

literature and could be readily explained by an increase in the Fermi energy level of the Au nanoparticles with an increase in their size, which was beneficial to the electron transfer (ET) to the substrates.[2, 5] In the presence of oxygen ([O_2] = 2.1 mM), photoirradiation of the Au/TiO_2 suspension containing DN-BODIPY resulted in a significantly decreased fluorescence intensity compared to that in an Ar-saturated atmosphere, indicating that the oxygen molecules acted as an effective electron scavenger (E_{red} = −0.63 V vs. NHE in acetonitrile),[6] which was unfavorable to the ET for the reduction of the DN-BODIPY on the surface.

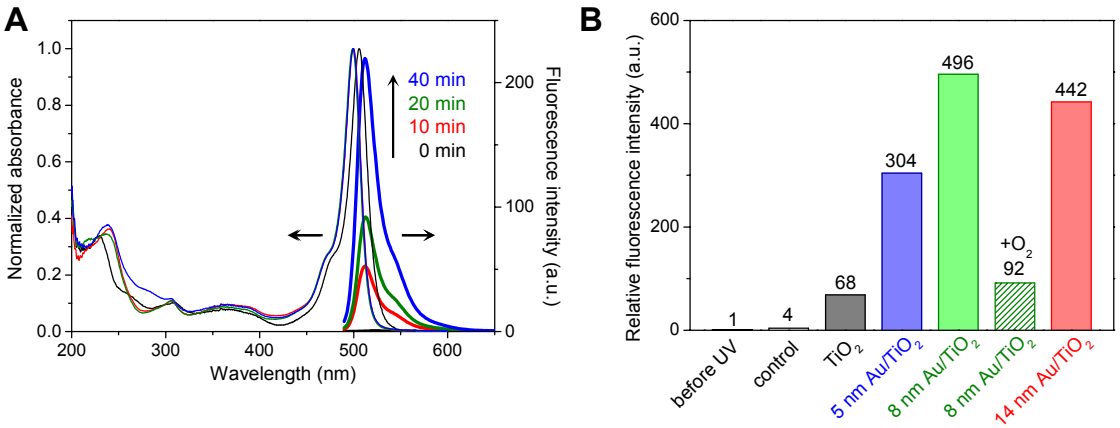

Fig. S2. (A) UV irradiation time dependence of absorption and fluorescence spectra of methanol solutions containing DN-BODIPY and 8 nm Au/TiO_2 particles. The inset is the magnified absorption peaks. (B) Relative fluorescence intensities measured before and after UV irradiation of the samples (1.0 g L^{-1}) containing DN-BODIPY (50 μM) for 30 min.

S4. Turnover rate of off-on cycle

Fig. S3A shows the time profiles for the turnover number (TON) of off-on cycles per 10 second over one Au/TiO_2 particle during 10 min of UV irradiation. It is easily seen that the photocatalytic activity of the same nanoparticle is temporally varying; however, the cumulative TON gradually increases with increasing UV irradiation time as shown in Fig. S3B. The turnover rate of off-on cycle (TOF) was defined as the first order derivative of cumulative TON with respect to time, and the resulting TOF values in each 10 second are given in Fig. 3A in the main text. To quantify the fluctuation of activity,

the mean value of turnover rate (<TOF>) and its relative standard derivation (RSD) during 10 min of UV irradiation was calculated as shown in Fig. 3B in the main text.

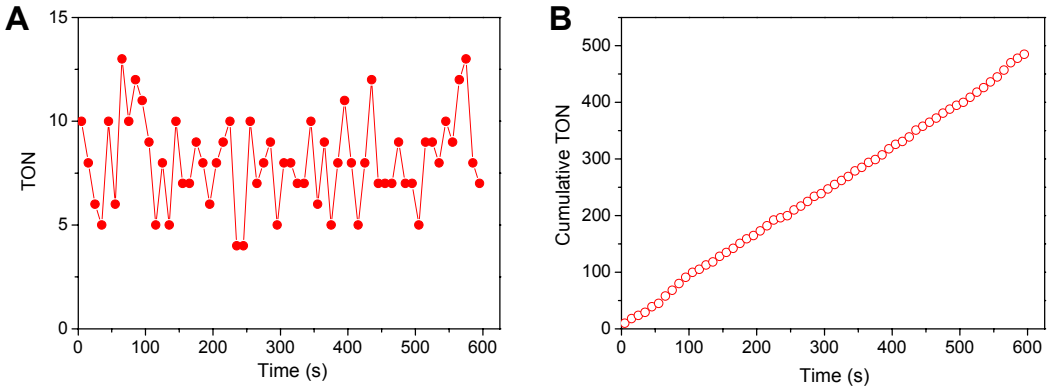

Fig. S3. (A) Number and (B) cumulative number of off-on turnovers every 10 second over a single 5 nm Au/TiO_2 particle ([DN-BODIPY] = 2.0 μM, I_{UV} = 0.5 W cm^{-2}).

S5. Influence of photoirradiation on the Au particle size

To examine the photothermal effect on the size of the Au nanoparticles during the course of the experiment, we performed non-contact mode atomic force microscopy (AFM) measurements. As shown in Fig. S4, we first confirmed the locations of an AFM cantilever and a 488-nm laser spot from optical transmission images of the AFM cantilever without (A) and with 488-nm laser and UV irradiation (B). Both the 488-nm CW laser (0.1 kW cm^{-2}) and UV light (365 nm, 0.5 W cm^{-2}) were then carefully irradiated onto the Au nanoparticle-modified TiO_2 surface for 10 min through an objective lens under the AFM tip. Note that the Au nanoparticles on the surface were immersed in Ar-saturated methanol during the photoirradiation. After the photoirradiation and solvent evaporation, the AFM tip was brought near the surface to capture AFM images of the Au nanoparticles.

Fig. S4C shows a typical AFM image obtained for Au nanoparticles (Aldrich, G1652) immobilized on the cover glass after 488-nm laser and UV irradiation for 10 min in Ar-saturated methanol. As illustrated in panel D, no obvious size change was observed when comparing the Au nanoparticles before and after photoirradiation. This result supports the conclusion that the fragmentation of the Au nanoparticles under photo-irradiation was likely negligible under the present experimental conditions.

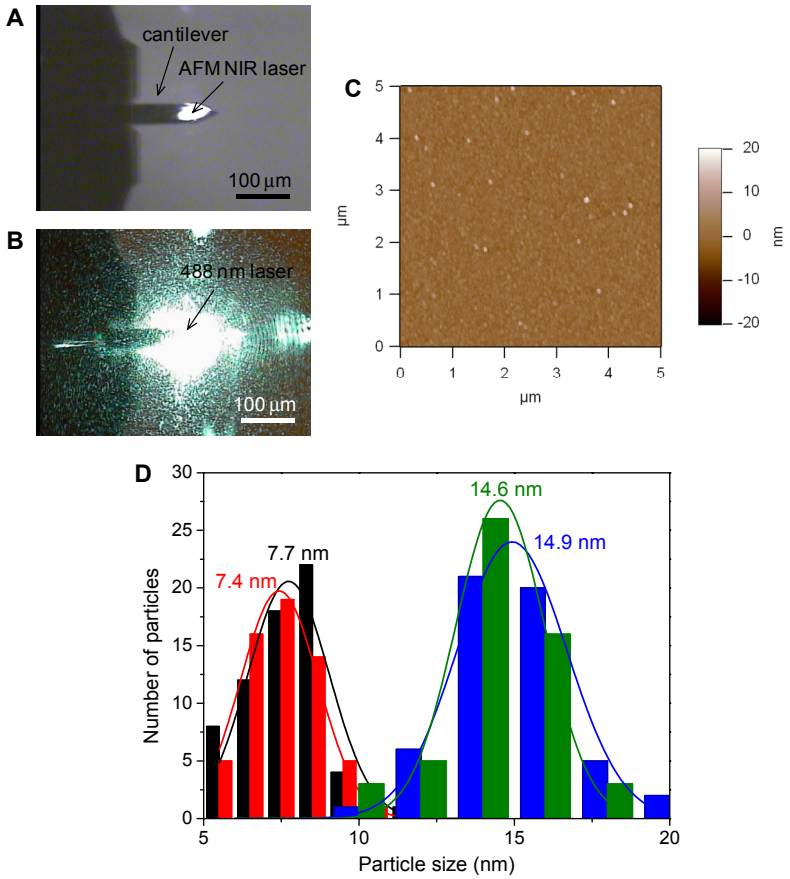

Fig. S4. (A, B) Optical transmission images of the AFM cantilever without (A) and with (B) 488-nm laser and UV irradiation. (C) A typical AFM image obtained for Au nanoparticles (Aldrich, G1652) immobilized on a cover glass after 488-nm laser and UV irradiation for 10 min in Ar-saturated methanol. (D) Histograms of the particle sizes obtained for two different sizes of Au nanoparticles (Aldrich, G1527 (black and red bars) and G1652 (blue and green bars)) immobilized on the TiO_2 surface before (black and blue bars) and after (red and green bars) 488-nm laser and UV irradiation for 10 min in Ar-saturated methanol. The solid lines indicate the Gaussian distributions fitted with the histograms.

S6. Size dependent of electron storage ability of Au nanoparticle

When one immobilizes Au nanoparticle on a conductive solid surface or nanoscaled semiconductor and uses them to enhance the interificial ET process, the key factors of the size dependence include not only the surface density of coordinatively unsaturated Au atom and electronic structure of nanoparticles, but also the charging–discharging properties of the particles. Especially, the size dependent double-layer charging of Au nanoparticles should be among the most fundamental factors to quantitatively control the ET characteristics. It has reported the double layer integral capacitance of Au surface per

unit area is ca. 70 μF cm^{-2} in aqueous solution, being independent of d_{Au} in the range of 3.7~40.8 nm.[7] Taking into account the dielectric constant of solvent, the hexanethiolate-coated Au particle with the diameter of 4.9 nm would have the capacitance of 2.0 aF, which is roughly consistent with the reported value (3.4 aF).[8] Thus, eqn. (S21) can approximately estimate the capacitance of Au nanoparticles with d_{Au} in the range of 3.7~40.8 nm. As shown in Table S1, when d_{Au} increases from 5.5 nm to 14.1 nm, the capacitance of Au particle in methanol increases from 2.8×10^{-17} F to 18.4×10^{-17} F, consequently the electron storage ability (q) of Au particle increases from 154 to 1014 electrons $particle^{-1}$.

$$C_{Au} = 70\ \mu F\ cm^{-2} \times A_{Au} \times (\varepsilon_{solvent} / \varepsilon_{water}) \quad \text{(S21)}$$

Table S1. Electron Storage Ability of Single Au Nanoparticle

Sample	d_{Au} (nm)	N_{Au} ($particle^{-1}$)	A_{Au} [a] (nm^2)	C_{Au} [b] (10^{-17} F)	q [c] (electrons $particle^{-1}$)
5 nm Au/TiO_2	5.5	22	95.0	2.8	154
8 nm Au/TiO_2	8.1	10	206.0	6.0	335
14 nm Au/TiO_2	14.1	3	624.3	18.4	1014

[a] Assuming that the surface area (A_{Au}) of one Au particle is the same as that of the sphere with a diameter of d_{Au}, $A_{Au} = 4\pi(d_{Au}/2)^2$. [b] Calculated from eqn. (S21), $\varepsilon_{water} = 78.5$, $\varepsilon_{methanol} = 32.7$, $\varepsilon_{hexanethiolate} = 3.0$ at 25 °C. [c] q is the number of electrons to be transferred to one Au particle to equilibrate with the excited TiO_2, $q = C_{Au} \times (E_F - E_F^*) \times 6.28 \times 10^{18}$ electrons $particle^{-1}$, in which Fermi levels of Au under dark (E_F) and photoexcited TiO_2 (E_F^*) is 0 V and −0.88 V vs. NHE in methanol, respectively.[9]

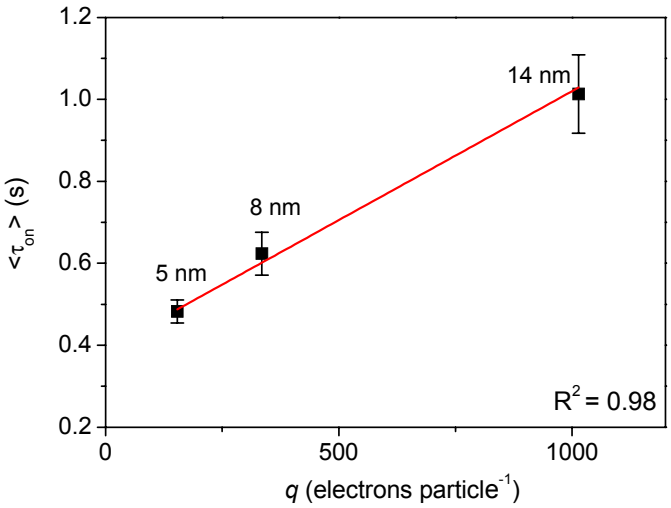

Fig. S5. Relationship between τ_{on} (I_{UV} = 0.5 W cm^{-2}) and electron storage ability of Au nanoparticle (q).

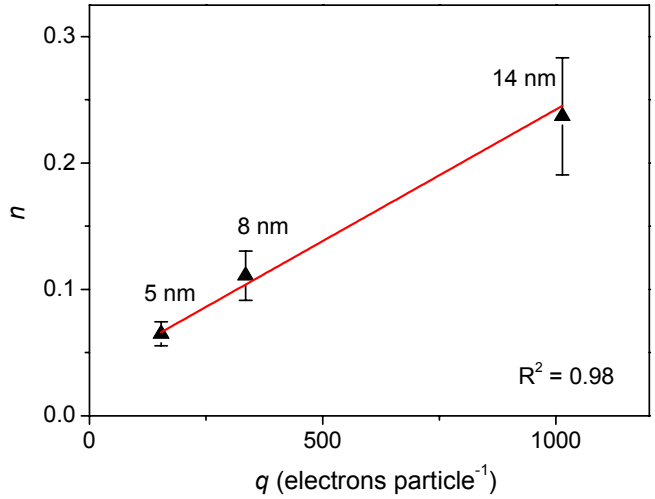

Fig. S6. Relationship between power coefficient (n, see eqn. (5) in the main text) and electron storage ability of Au nanoparticle (q).

S7. Kinetic analysis of Au/TiO_2 photocatalytic reactions

The reaction equations for the photocatalytic reduction of DN-BODIPY over Au/TiO_2 are described in eqns (S1)–(S8). The accumulation of electrons in Au particle increases its Fermi energy at photostationary state (E_F^*) step by step until E_F^* exceeds the reduction potential of DN-BODIPY, which is called the charging process of Au. As soon as just any one of Au nanoparticles accomplishes the charging process, the photocatalytic reduction of DN-BODIPY will be triggered concomitantly with

turning on fluorescence. Thus, the ET through nanocomposite interfaces should be resolved into that between single TiO_2 nanoparticle and several individual Au nanoparticles. The overall ET reaction in one TiO_2 particle consists of all the parallel reactions for N_{Au} individual Au nanoparticles.

$$\mathrm{Au/TiO_2 + DN\text{-}BODIPY} \overset{K_{ad}}{\rightleftharpoons} \mathrm{DN\text{-}BODIPY_{ad}} \qquad [\mathbf{S}_{ad}] = K_{ad}[\mathbf{S}]/(1+K_{ad}[\mathbf{S}]) \qquad \text{(S1)}$$

$$\mathrm{Au/TiO_2} + h\nu \xrightarrow{I_{UV}\varphi} \mathrm{h^+_{VB}(TiO_2) + e^-_{CB}(TiO_2)} \qquad v_1 = I_{UV}\varphi \qquad \text{(S2)}$$

$$\mathrm{h^+_{VB}(TiO_2) + e^-_{CB}(TiO_2)} \xrightarrow{k_{rec}} \mathrm{heat} \qquad v_2 = k_{rec}[\mathrm{h^+_{VB}}][\mathrm{e^-_{CB}}] \qquad \text{(S3)}$$

$$\mathrm{h^+_{VB}(TiO_2) + CH_3OH_{ad}} \xrightarrow{k_{ox,1}} \mathrm{^{\bullet}CH_2OH_{ad} + H^+} \qquad v_3 = k_{ox,1}[\mathrm{h^+_{vb}}][\mathrm{CH_3OH_{ad}}] \qquad \text{(S4)}$$

$$\mathrm{^{\bullet}CH_2OH_{ad}} \xrightarrow{k_{ox,2}} \mathrm{HCHO + H^+ + e^-_{CB}(TiO_2)} \qquad v_4 = k_{ox,2}[\mathrm{^{\bullet}CH_2OH_{ad}}] \qquad \text{(S5)}$$

$$\mathrm{e^-_{CB}(TiO_2)} \xrightarrow{k_{et}} \mathrm{e^-_{Au}(Au)} \qquad v_5 = k_{et}[\mathrm{e^-_{CB}}][R_s] \qquad \text{(S6)}$$

$$\mathrm{e^-_{CB}(TiO_2)} \xrightarrow[\text{overall}]{k_{et}} \mathrm{e^-_{Au}(Au)} \qquad v_6 = N_{Au}v_5 = N_{Au}k_{et}[\mathrm{e^-_{CB}}][R_s] \qquad \text{(S7)}$$

$$\mathrm{4e^-_{Au}(Au) + DN\text{-}BODIPY_{ad} + 4H^+} \xrightarrow{k_{red}} \mathrm{HN\text{-}BODIPY_{ad} + H_2O} \qquad v_7 = k_{red}[\mathbf{S}_{ad}] \qquad \text{(S8)}$$

Where I_{UV} is the incident UV light intensity, φ is the integrated absorption fraction over the given wavelength range, the subscript "ad" refers to adsorption, and $[R_s]$ is the concentration of the surface reactive sites that trap the electrons on one Au nanoparticle.

Under steady-state conditions, we have that

$$\frac{\mathrm{d}[\mathrm{h^+_{VB}}]}{\mathrm{d}t} = v_1 - v_2 - v_3 = 0 \qquad \text{(S9)}$$

$$\frac{\mathrm{d}[\mathrm{e^-_{CB}}]}{\mathrm{d}t} = v_1 - v_2 + v_4 - v_6 = 0 \qquad \text{(S10)}$$

$$\frac{\mathrm{d}[\mathrm{^{\bullet}CH_2OH_{ad}}]}{\mathrm{d}t} = v_3 - v_4 = 0 \qquad \text{(S11)}$$

$$\frac{\mathrm{d}[\mathrm{e^-_{Au}}]}{\mathrm{d}t} = v_7 - v_5 = 0 \qquad \text{(S12)}$$

Combining eqns. (S9), (S10), and (S11), we can obtain that

$$[\mathrm{h^+_{VB}}]_{ss} = \frac{N_{Au}k_{et}[\mathrm{e^-_{CB}}][R_s]}{2k_{ox,1}[\mathrm{CH_3OH_{ad}}]} \qquad \text{(S13)}$$

By substituting eqn. (S13) into eqn. (S9), the following equation is obtained

$$2k_{ox,1}I_{UV}\varphi[CH_3OH_{ad}] = N_{Au}k_{rec}k_{et}[R_s][e^-_{CB}]^2 + N_{Au}k_{et}k_{ox,1}[CH_3OH_{ad}][R_s][e^-_{CB}] \quad (S14)$$

For very low light intensities, the first term in eqn. (S14) is much smaller than the second term; conversely, the second term would be neglected at very high carrier concentration (i.e. high light intensities). Thus the eqn. (S14) can be simplified to

$$[e^-_{CB}]_{ss} = \frac{2I_{UV}\varphi}{N_{Au}k_{et}[R_s]} \quad \text{(low } I_{UV}\text{)} \quad (S15)$$

$$[e^-_{CB}]_{ss} = \left(\frac{2k_{ox,1}[CH_3OH_{ad}]I_{UV}\varphi}{N_{Au}k_{rec}k_{et}[R_s]}\right)^{1/2} \quad \text{(high } I_{UV}\text{)} \quad (S16)$$

If $K_{ad}[\mathbf{S}] > 1$, the eqn. (S8) becomes

$$v_7 = k_{red}[\mathbf{S}_{ad}] = \frac{k_{red}K_{ad}[\mathbf{S}]}{1+K_{ad}[\mathbf{S}]} \approx k_{red} \quad (S17)$$

From eqns. (S6), (S12), and (S17), the following equation is obtained

$$\frac{d[HN\text{-}BODIPY_{ad}]}{dt} = <\tau_{off}>_s^{-1} \times A_{Au} = k_{red} = k_{et}[e^-_{CB}][R_s] \quad (S18)$$

Finally, by substituting eqns. (S15) and (S16) into eqn. (S18), the following expressions for the reduction rate of DN-BODIPY over Au/TiO_2 can be obtained

$$<\tau_{off}>_s^{-1} = \frac{2I_{UV}\varphi}{N_{Au}A_{Au}} \quad \text{(low } I_{UV}\text{)} \quad (S19)$$

$$<\tau_{off}>_s^{-1} = \frac{1}{A_{Au}}\left(\frac{2k_{ox,1}k_{et}[R_s][CH_3OH_{ad}]I_{UV}\varphi}{N_{Au}k_{rec}}\right)^{1/2} \quad \text{(high } I_{UV}\text{)} \quad (S20)$$

S8. References

1. T. Tachikawa, N. Wang, S. Yamashita, S.-C. Cui and T. Majima, *Angew. Chem. Int. Ed.*, 2010, **49**, 8593-8597.
2. T. Kiyonaga, T. Mitsui, M. Torikoshi, M. Takekawa, T. Soejima and H. Tada, *J. Phys. Chem. B*, 2006, **110**, 10771-10778.
3. K. Naito, T. Tachikawa, M. Fujitsuka and T. Majima, *J. Am. Chem. Soc.*, 2009, **131**, 934-936.
4. T. Tachikawa and T. Majima, *Langmuir*, 2009, **25**, 7791-7802.
5. T. Kiyonaga, M. Fujii, T. Akita, H. Kobayashi and H. Tada, *Phys. Chem. Chem. Phys.*, 2008, **10**, 6553-6561.

6. D. T. Sawyer, G. Chiericato, Jr., C. T. Angelis, E. J. Nanni, Jr. and T. Tsuchiya, *Anal. Chem.*, 1982, **54**, 1720-1724.
7. A. Toyota and T. Sagara, *Electrochim. Acta*, 2008, **53**, 2553-2559.
8. J. Kim and D. Lee, *J. Am. Chem. Soc.*, 2007, **129**, 7706-7707.
9. G. Redmond and D. Fitzmaurice, *J. Phys. Chem.*, 1993, **97**, 1426-1430.